

High performance of ultrasonic-assisted synthesis of two spherical polymers for enantioselective catalysis

Zahra Sharifzadeh¹, Kayhaneh Berijani¹, Ali Morsali^{*}

Department of Chemistry, Faculty of Sciences, TarbiatModares University, P.O. Box 14117-13116, Tehran, Islamic Republic of Iran

ARTICLE INFO

Keywords:

Chiral magnetic composite-based capsules
Sonochemical irradiation
Green sustainable catalysts
Acid-base bifunctional catalysts
Asymmetric catalysis

ABSTRACT

Chiral polymers have aroused great attention in among chiral supramolecular materials based on their features. Herein, for the first time, the synthesis of chiral polymeric composites (CMNPs/1,4-Zbtb & 1,3-Zbtb) have been reported with entrapment through three strategies: ultrasonic irradiation, solvothermal, and mechanical stirring. According to the obtained results, it is found that ultrasound-assisted synthesis can be considered as an inexpensive and efficient method than the others, from the point of view of energy and time consuming. In this strategy, encapsulation of chiral magnetic nanoparticles (CMNPs) by using tetrazole-based polymers (Zbtbs) happens, in-situ. These chiral sphere-like inorganic-organic polymers can be considered as core and shell composites with catalytic activity due to their acidic (semi unsaturated Zn: open metal sites) and basic (abundant basic nitrogens) centers. In these structures, the unprecedented chirality induction can happen from the core to shell by non-covalent interaction, easily. They could catalyze symmetric oxidation and asymmetric Henry condensation to give chiral β -nitroalkanol. Circular dichroism and chiral gas chromatography were used to characterize the produced enantiomers. These chiral polymeric materials can be considered as unique acid-base bifunctional catalysts with efficient properties such as high stability, enantiomeric excess, enantioselectivity to the main product, and protecting from CMNPs leaching.

1. Introduction

The existence of chirality in living systems and material science is one of the reasons for research in this field [1–6]. Considering the numerous applications of chiral materials such as pharmacy, magnetism, enantioselective separation, and nonlinear optics, exploring their potential for asymmetric catalysis have been also developed. These abilities will surely motivate the researchers to devote much research effort on synthesis [7–11].

Generally, producing chiral materials especially at the supramolecular level can happen by enantiopure reagent [12,13] or spontaneous resolution [14–18]. In contrast to the above-mentioned strategies, using chiral external agent is a fast, low-cost and controllable pathway for chiralization of supramolecular especially metal-organic hybrid materials and chiral coordination polymers (CCPs) [19–24]. Until now, a lot of chiral catalysts have been successfully developed [25–27] such as polymer-supported chiral catalysts but lack of protection of chiral species is one of the disadvantages that it should be regarded. Since there are weaknesses in these catalytic systems such as leaching and

decreasing of catalysts activity than their homogeneous counterparts. There is a method to solve problems: encapsulation strategy. This approach can be proposed and designed due to the production of the core-shell polymeric capsules [28]. Usually, this method entails the following requirements: use of a stabilizing agent (e.g. surfactants) [29,30] or functional linker in host synthesis [31], however these factors are not always possible to use. Among other protective agents as host, infinite coordination polymers (ICPs) can be good options due to their dependent properties [32–37]. Mirkin's groups, Dong, and Wang are pioneers of ICPs development by using different bifunctional ligands [32]. In the following years, the synthesis of homochiral ICPs was investigated by using chiral salen-based ligand, for the first time [38]. Regarding the topic of porosity in ICPs, it should be mentioned that in contrast to porous coordination polymers as well as metal-organic frameworks, infinite coordination polymers lack acceptable porosity. Indeed, crystalline MOFs showed fairly good gas storage, separations, and heterogeneous catalysis owing to their high porosity and large surface areas. While in ICPs are amorphous supramolecular particles that self-assembled in mild conditions. So, due to the lack of growth of regular

* Corresponding author.

E-mail address: morsali_a@modares.ac.ir (A. Morsali).

¹ These two authors contributed equally to this work.

<https://doi.org/10.1016/j.ultsonch.2021.105499>

Received 12 December 2020; Received in revised form 2 January 2021; Accepted 16 February 2021

Available online 20 February 2021

1350-4177/© 2021 The Author(s).

Published by Elsevier B.V. This is an open access article under the CC BY-NC-ND license

(<http://creativecommons.org/licenses/by-nc-nd/4.0/>).

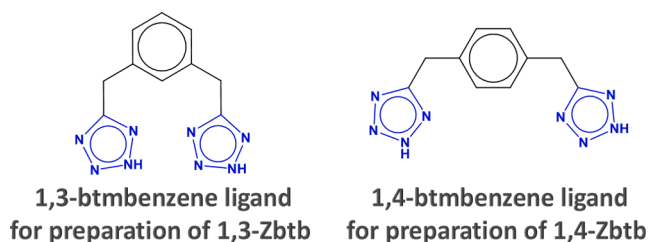


Fig. 1. A view of the molecular structure of 1,3- and 1,4-btmbenzene.

crystalline plates and a well-defined framework, porosity in these compounds is usually not observed or is reported in small amounts [56,57]. However, according to the nature of ICPs structure, their physical and chemical properties, they can be served as a good candidates in gas storage, mixture separations, asymmetric catalysis, and biosensing [37], but from 2006 to now, only one ICP has been reported with catalytic activity [36]. Until now, many chiral polymers have been explored, [39–42] but so far, no chiral ICP has been reported by induction method. In our previous work, we reported two strong tetrazolyl infinite coordination polymers by using 1,3-btmbenzene and 1,4-btmbenzene (Fig. 1) with hollow sphere morphology through three methods including solvothermal, ultrasonic irradiation, and mechanical stirring [43–45]. Herein, for the first time, we prepared two chiro-magnetic nanoparticles/polymer composites (CMNPs/Zbtb) with the assistance of ultrasonic irradiation. Among the above-mentioned synthetic methods for the preparation of chiral magnetic capsules, we chose the sonochemical method as a simple, fast, environmental, and low-cost strategy [46,47]. Ultrasound (US) has an important effect on the synthesis of our spherical polymers because we observed that in the other methods, no core-shell polymer was obtained through the mixing of Zn, btb, and CMNPs. From past investigations to date, ultrasonic irradiation shows a vital role in the synthesis of metal-organic polymers and frameworks [48–50]. In general, several methods have been introduced to perform chemical reactions. Most of these methods are based on

heating the precursors to reach the desired product. Although, some of them have problems such as long reaction time, non-satisfactory yields, more solvent, toxic/costly reagents, and high temperatures [51,52]. It seems that ultrasonic as a non-conventional energy source can be a good alternative to conventional energy sources [53]. Moreover, ultrasound waves can provide the conditions for achieving smaller sizes of metal-organic polymers and frameworks in milder conditions without the need for high temperature and long time. So far, ultrasound as a major agent in synthesis has been used in the creation of many materials due to reducing time, producing higher surface area, crystallinity, and pore volume [54,55].

To explain the effect of ultrasound waves on the synthesis of metal-organic supramolecular, we should mention that the US can affect in the heterogeneous systems, chemically, and mechanically. Chemical and mechanical effects are related to the presence of high temperature and strong shear gradients, respectively. The localized hot spots with exceedingly high transient temperatures promote chemical reactions and the formation of nano-sized structures as results of acoustic cavitation within collapsing bubbles. In other words, cavitation (bubbles formation, growth and collapsing) in ultrasonic bath, can be considered as the main factor for these chemical and physical effects, and acoustic cavitation is also responsible for promoting organic reactions [53]. During this mechanism (ultrasonic irradiation) the migration of nanoparticles and self-assembly of metal-organic polymer are accelerated. It should also be noted that the consequences of the cavitation are many times more common in heterogeneous systems than homogeneous ones [56,57]. However, the number of published articles about preparation of polymers by ultrasonic irradiation is not low but they are limited in the synthesis of composites. PTA-MIL-53(Fe) [58], $\text{Fe}_3\text{O}_4\text{/TMU-17-NH}_2$ [59], and Lipase@ZIF-8 by Rathod [60] are some examples of ultrasound irradiated composites. Recently, we also reported a chiral magnetic MOF as a basic framework that was synthesized via the sonochemical method [61].

So, we aimed to use the present stable tetrazole-based polymers (1,3-Zbtb & 1,4-Zbtb as the shell) as nitrogen-rich conjugated materials for

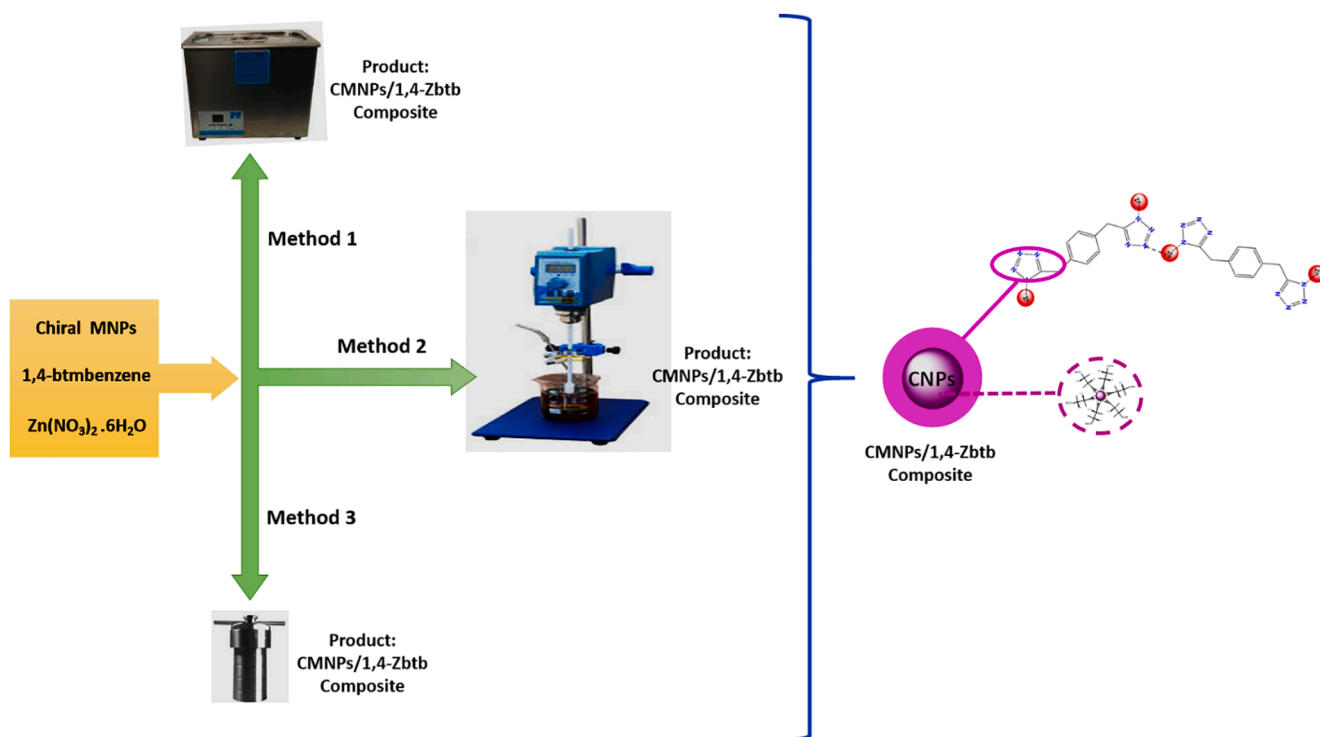


Fig. 2. Schematic demonstration for the synthetic routes of chiral green composite (CMNPs/Zbtbs). (For interpretation of the references to colour in this figure legend, the reader is referred to the web version of this article.)

the synthesis of stable chiral catalysts and asymmetric catalysis owing to their features such as polarity, basicity, and large cavity. They have stable catalytic centers in their structures and in fact, they are not an inert material. To chiralize active surfaces of these polymers, we have also chosen CMNPs as the core, [62,63] that are prepared by using L-(+)-tartaric acid (chiral carboxylic acid) stabilized nano-magnetite with high chirality induction [64]. As above mentioned, three synthetic methods were employed to synthesize these chiral magnetic materials by encapsulation of CMNPs. The results showed that the best method is using ultrasonic irradiation. However, in several reports, the effect of ultrasonic in encapsulation of various molecules has been shown and proved [48,58,65,66]. In fact, carrying out reactions in ultrasonic-bath not only leads to the dispersion of magnetic NPs and especially magnetic NPs, but also causes accelerates binding of metal to organic linkers around NPs. Therefore, we observed that in the absence of ultrasonic irradiation, functionalized-Fe₃O₄ nanoparticles definitely cannot well disperse well and the majority of them are located on the outer surface of hollow spherical polymers. The produced catalysts by sonochemical synthesis have smaller dimension and higher active surface than two other synthetic methods. So, these features can induce high catalytic performance to chiral ICPs and show the effect of ultrasonic irradiation on the structure, respectively. Fig. 2 shows the schematic diagram of the preparation process for CMNPs/1,4-Zbtb as the main catalyst. Since, it showed better results than CMNPs/1,3-Zbtb, preserving its structural integrity and catalytic activity (synthesis of CMNPs/1,3-Zbtb similar to CMNPs/1,4-Zbtb). Apart from the presence of unsaturated Zn atoms at the shell that can act as active acidic centers in the oxidation, nitroaldole reaction (as a type of C–C bond-forming) reaction can be proceeded by Lewis-acid or base [67–71]. To the best of our knowledge, this is the first example of chiral ICP in asymmetric catalysis with high enantiomeric excess [72,73] by chiral agent protection.

2. Experimental section

2.1. Materials and instrumentation

Materials: L-(+)-Tartaric acid ((2R,3R)-(+)-tartaric acid, >99%, Merck), iron(III) chloride hexahydrate (FeCl₃·6H₂O, 98% Fluka), diethylene glycol (99%, Merck), 1,4-phenylenediacetonitrile and 1,3-phenylenediacetonitrile were purchased from Sigma-Aldrich (Milwaukee, WI, USA). Sodium azide and zinc bromide were commercially obtainable from Merck Company (Darmstadt, Germany) and other reagents and solvents were purchased and used without further purification from commercial suppliers (Sigma Aldrich, Alfa Aesar, TCI, and others).

IR spectra were recorded using a Nicolet 100 Fourier Transform IR spectrometer in the range of 500–4000 cm⁻¹ using the KBr disk technique. The inductively coupled plasma (ICP) analyses were achieved on a Varian ICP-OES VISTA-PRO CCD instrument. Melting points were measured on an Electrothermal 9100 apparatus. UV–vis absorption spectra were obtained by UV–vis Perkin Elmer Lambda 25 spectrophotometer. CD spectra were recorded on a Jasco J-715 spectropolarimeter (Japan). Gas chromatography (GC) runs were performed on an Echrom GC A90 gas chromatograph. The samples were also characterized by using a field emission scanning electron microscope (FE-SEM) TESCAN MIRA with gold coating. TEM (transmission electron microscopy) analysis was performed on a JEOL 2100 electron microscope at an operating voltage of 200 kV. Powder X-ray diffraction (PXRD) measurements were performed using a Philips X'pert diffractometer with monochromated Cu-K α ($\lambda = 1.54056 \text{ \AA}$) radiation. The contact angle was measured by using an OCA 15 plus apparatus. Magnetic measurements were performed with a Quantum Design vibrating sample magnetometer (VSM) at room temperature in an applied magnetic field sweep. Ultrasonic generation was carried out in an ultrasonic bath SONICA-2200 EP (frequency of 40 kHz). The sonicator used in this study was a SONICA-2200 EP with adjustable power output (maximum 305 W

at 40/60 kHz). A horn-type tube Pyrex reactor was custom-made and fitted to the sonicator bath.

3. Preparation of CMNPs/1,3-Zbtb & CMNPs/1,4-Zbtb composites via solvothermal strategy.

The CMNPs (as reported in S1) (0.04 mmol) were well dispersed (10 mL DMF) by ultrasonic irradiation. Then the solution of 1,4-btmbenzene ligand (1 mmol) (or 1,3-btmbenzene, S2) in DMF (15 mL) and methanolic solution (5 mL) of Zn(NO₃)₂·6H₂O (296 mg, 1 mmol) were added to dispersed nanoparticles. This mixture was transferred to a 30 mL Teflon-lined stainless-steel vessel, sealed, and heated at 120 °C for 12 h.

3.1. Preparation of CMNPs/1,3-Zbtb & CMNPs/1,4-Zbtb composites via mechanical stirring method

The CMNPs (0.04 mmol) were fully dispersed in DMF (10 mL) by ultrasonic irradiation. Then the solution of 1,4-btmbenzene ligand (1 mmol) (or 1,3-btmbenzene, S2) in DMF (15 mL) was added to it. Then, during stirring by a mechanical stirrer, a methanolic solution (5 mL) of Zn(NO₃)₂·6H₂O (296 mg, 1 mmol) was added dropwise to them. After stirring for one hour, the produced product was separated and washed with methanol and DMF.

3.2. Preparation of CMNPs/1,3-Zbtb & CMNPs/1,4-Zbtb composites by using of ultrasonic irradiation

The CMNPs (0.04 mmol) was dispersed well in DMF (10 mL) by use of ultrasonic irradiations. Then the solution of 1,4-btmbenzene ligand (1 mmol) in DMF (15 mL) was added to dispersed nanoparticles and then both of them were sonicated for specific times (30–45 min) at room temperature. After homogenization, a methanolic solution (5 mL) of Zn(NO₃)₂·6H₂O (296 mg, 1 mmol) was added dropwise to the mixture of CMNPs and ligand in the ultrasonic bath. Subsequently, the light-brown micro sphere-like polymers as shell with chiral magnetic nanoparticles within their core were generated. Finally, they were purified by magnetic separation and washed with DMF through filtration-redispersion cycles. IR data (v/cm⁻¹): 427 (s), 657 (w), 777 (w), 1106 (w), 1430 (m), 1658 (s), 1732 (s), 2349 (w), 2830 (w), 2935 (w), 3428 (m). Preparation of CMNPs/1,3-Zbtb was similar to CMNPs/1,4-Zbtb without any change in ratios. IR data (v/cm⁻¹): 446 (w), 690 (w), 765 (m), 1108 (m), 1434 (m), 1653 (s), 1730 (s), 2351 (w), 2810 (m), 2920 (m) and 3430 (m).

3.3. Typical reaction procedure of Henry reaction

In a typical reaction, chiral catalyst (CMNPs/1,3-Zbtb & CMNPs/1,4-Zbtb) (0.05 g) was added to a solution of MeOH (5 mL) in 5 mL screw-capped vial. Afterwards, benzaldehyde (2 mmol) and nitromethane (5 mmol) were added into above solution. The reaction mixture was allowed to stir at 70 °C. After that, upon filtration by an external magnet, the catalyst was separated and washed with MeOH. The solution was collected and analyzed by chiral GC.

3.4. Recycling of catalyst

After the first step of the catalytic cycle, the heterogeneous catalyst was separated by external magnet, rinsed several times by MeOH and dried for 5 h in oven (80 °C). Then, the recovered catalyst was reused in the subsequent recycling experiments under identical reaction conditions.

3.5. Typical reaction procedure of benzyl alcohol oxidation to benzaldehyde

In a typical procedure, BzOH (2 mmol) and deionized water (5 mL),

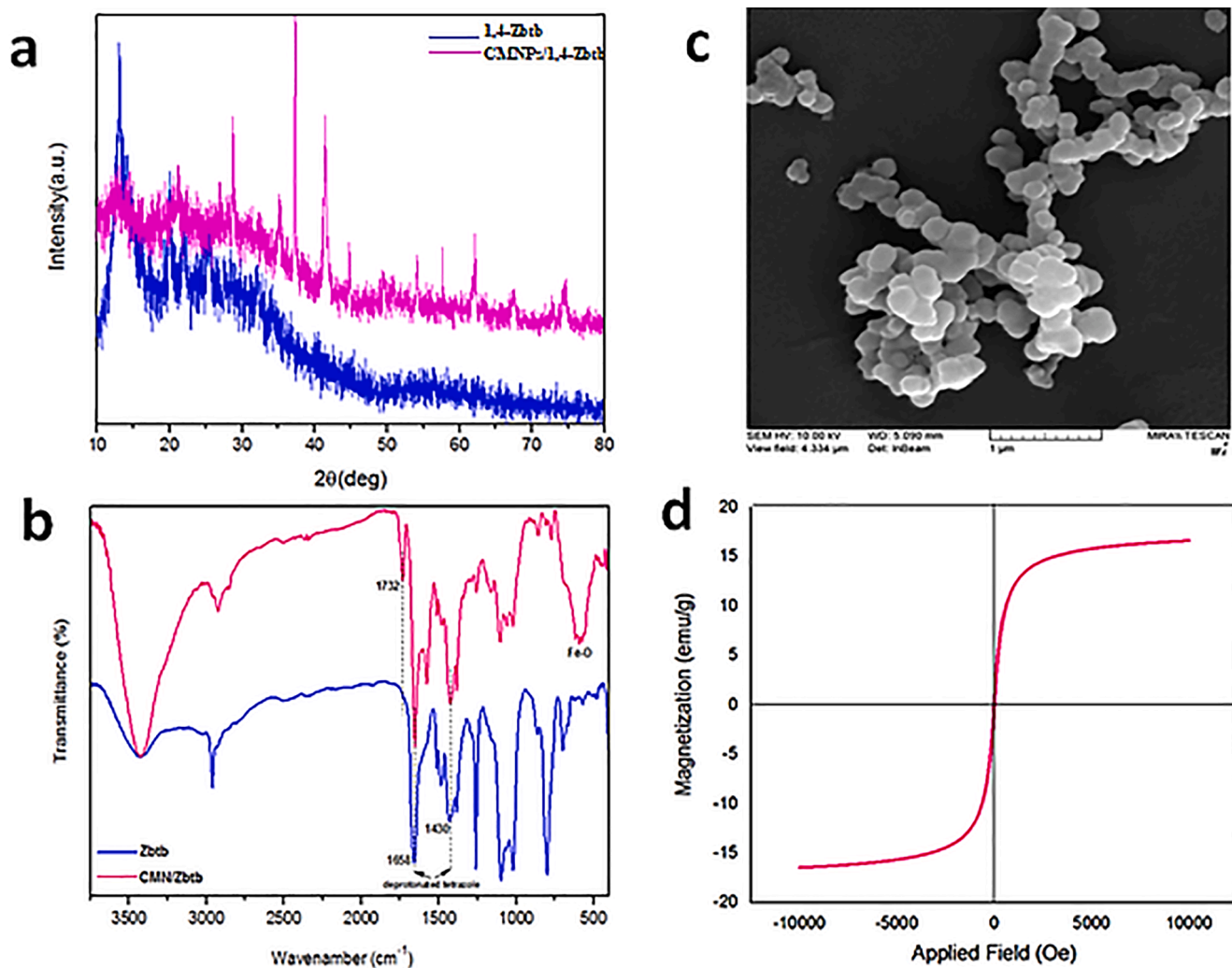


Fig. 3. (a) PXRD patterns, (b) FTIR spectra of hollow 1,4-Zbtb capsule and CMNPs/1,4-Zbtb, respectively. (c) SEM image of CMNPs/1,4-Zbtb and (d) Magnetization curve of CMNPs/1,4-Zbtb. Synthesis method: ultrasonic irradiation.

and were added to a 25 mL two-neck flask containing magnetic catalyst (0.025 g). This system was equipped with a condenser. The reaction mixture was vigorously stirred at 85 °C for 5 h and H₂O₂ (5 mmol, 30 wt % in water) was added dropwise in three steps. Then, the solid catalyst was separated from the reaction mixture by an external magnet. The product was extracted by ethyl acetate (5 mL), washed with saturated sodium thiosulfate solution (2 × 3 mL) and analyzed by a gas chromatography system.

4. Results and discussion

4.1. Characterization of chiral magnetic composites (CMNPs/Zbtbs)

In this research work, the catalytic results showed that the efficiency of the optimized chiral catalyst through ultrasonic irradiation is very sensible. In the following, the further observations are used to support this claim. The generation of our novel chiral polymeric composites (CMNPs/Zbtbs) is done in two steps: in first step, tartaric acid as chiral inducer was stabilized on Fe₃O₄ nanoparticle. In next step, Fe₃O₄-tartaric acid nanoparticles were dispersed in solution by the help of ultrasonic irradiations, and eventually they were encapsulated within Zbtb colloidal particles through in situ method, in a few minutes (Fig. 2). We previously characterized our sphere-like polymer structures with different methods. On the other hand, our purpose in this report was the introduction of the best chiral Lewis base to the promotion of

asymmetric nitroaldol reaction. As we discussed and showed in the following, CMNPs/1,4-Zbtb worked better than compared to CMNPs/1,3-Zbtb. So, our optimized catalyst was CMNPs/1,4-Zbtb and specific characterization about it was carried out. It should also be noted that due to the high structural similarities of the two ICPs, almost identical results in early characterization are not unexpected, although full characterization about Fe₃O₄/1,3-Zbtb was carried out in our previous work [43–45]. Powder x-ray diffraction (PXRD) pattern was used first as direct evidence to confirm the formation of CMNPs/1,4-Zbtb. For this purpose, powders of 1,4-Zbtb, CMNPs/1,4-Zbtb, and CMNPs nanoparticles are deposited in the hollow of a silicon zero-background plate 0.2 mm deep (PW1812, Philips company). The diffractometer of this apparatus equipped with an X-ray tube (CuK α , $\lambda = 1.5418 \text{ \AA}$), and the generator was set at 40 kV and 40 mA (2 θ range: from ~10 to 80°). The comparison of CMNPs/1,4-Zbtb with hollow 1,4-Zbtb revealed that polymer preserved its amorphousness and several reflections appeared at $2\theta = 30.3^\circ, 35.4^\circ, 43.2^\circ, 53.5^\circ, 57.2^\circ$ and 62.9° corresponding to Fe₃O₄ in XRD-pattern matched well with the presence of Fe₃O₄ (Fig. 3a) [74]. PXRD pattern of CMNPs showed that intensity of Fe₃O₄ peaks decreases due to functionalization of Fe₃O₄ by tartaric acid. Also, in comparison of XRD-patterns of the as-prepared composites by all three methods, no noticeable differences were observed (Fig. S9).

About 1,3-Zbtb and CMNPs/1,3-Zbtb, similar to 1,4-Zbtb and CMNPs/1,4-Zbtb, powder x-ray diffraction analysis was also performed to prove the existence of CMNPs in composite form with polymeric

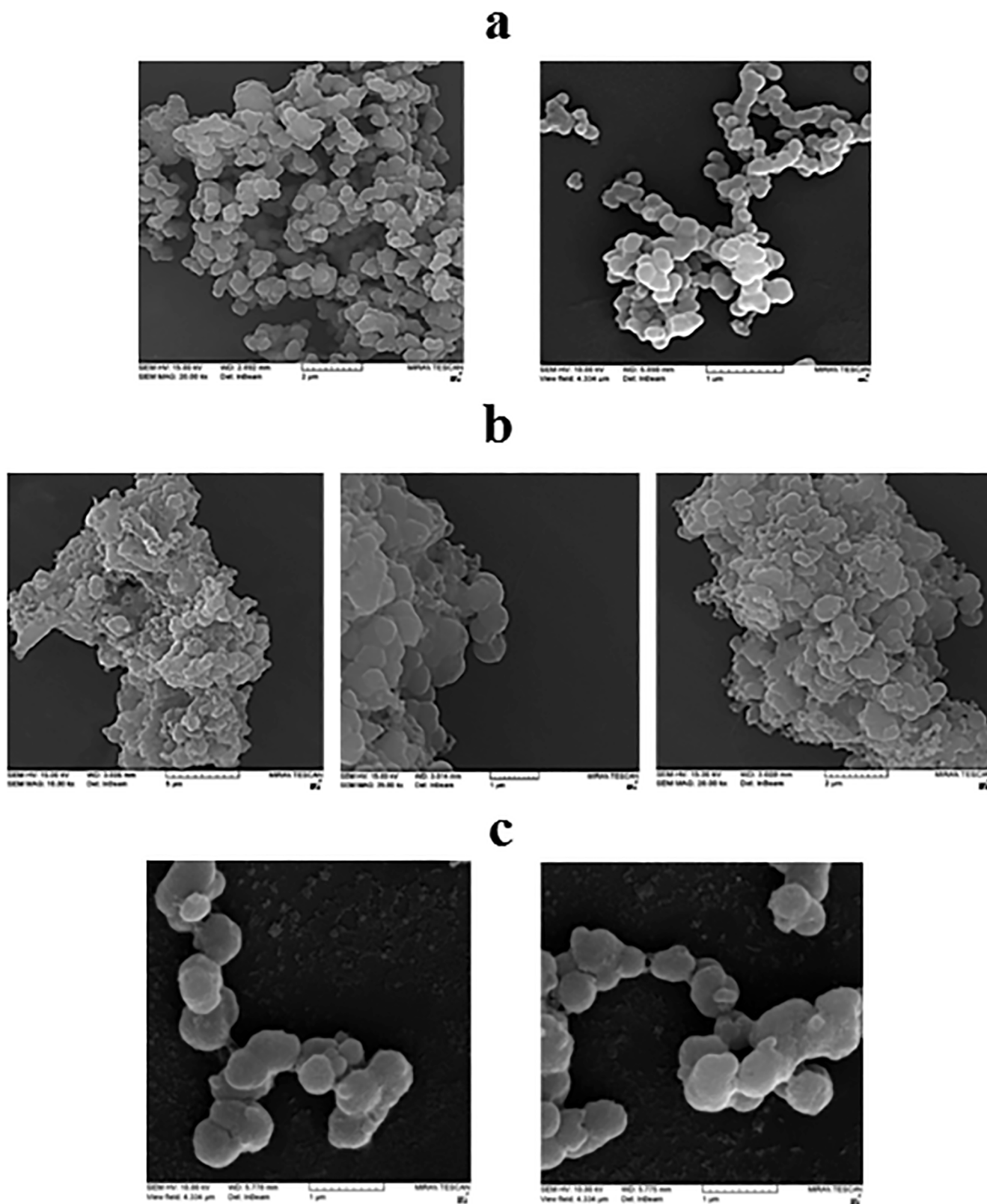
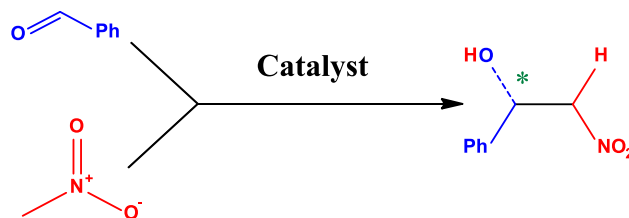


Fig. 4. SEM images of the synthesized CMNPs/1,4-Zbtb by (a) ultrasonic irradiation, (b) solvothermal method, and (c) mechanical stirring.

capsules (Figs. S9 and 3a) [43]. Despite all the knowledge about poor porosity in ICPs, we examined the uptake of N_2 gas for our desired composition. As expected, we obtained a very low N_2 BET surface area (close to zero) which proved the non-porosity of our structure. The 1,4-Zbtb modification was inspected by Fourier transform infrared

spectroscopy (FTIR) (Fig. 3b). Comparing FTIR spectra both of hollow 1,4-Zbtb capsule and CMNPs/1,4-Zbtb revealed the presence of the characteristic C=O stretching band of tart at 1732 cm^{-1} corresponding to chemisorption of tartaric acid on the surface of Fe_3O_4 [75] in CMNPs/1,4-Zbtb. Carbon-oxygen stretching of tartaric acid carboxylate groups

Table 1
Optimization of Henry reaction conditions.^a



Entry	Catalyst	Solvent	Temperature(°C)	Time (h)	Conversion (%)	Selectivity ^b (%)	Ee ^c (%)
1	CMNPs/1,4-Zbtb	MeOH	70	2	15	80	23(S)
2	CMNPs/1,4-Zbtb	MeOH	70	5	26	78	51(S)
3	CMNPs/1,4-Zbtb	MeOH	70	10	58	82	78(R)
4	CMNPs/1,4-Zbtb	MeOH	70	12	85	81	90(R)
5	CMNPs/1,4-Zbtb	MeOH	40	12	20	72	46(S)
6	CMNPs/1,4-Zbtb	Water	70	12	19	42	39(S)
7	CMNPs/1,4-Zbtb	EtOH	70	12	9	49	41(R)
8	1,4-Zbtb ^d	MeOH	70	12	80	78	–
9	CMNPs/1,3-Zbtb	MeOH	70	10	51	73	70(R)
10	CMNPs/1,3-Zbtb	MeOH	70	12	75	77	85(R)
11	CMNPs/1,3-Zbtb	Water	70	12	15	45	40(R)
12	CMNPs/1,3-Zbtb	EtOH	70	12	7	35	28(S)
13	1,3-Zbtb ^d	MeOH	70	12	69	75	–
14 ^e	CMNPs/1,4-Zbtb	MeOH	70	12	35	69	61
15 ^f	CMNPs/1,4-Zbtb	MeOH	70	12	63	78	79

^a unless otherwise specified, all reactions were conducted with 5 mmol of nitromethane, 2 mmol of benzaldehyde, 5 mL of solvent, and 0.05 g of catalyst in the ultrasonic bath.

^b Related to nitroalcohol product.

^c Enantiomeric excess of major isomer was determined by GC analysis using a chiral column.

^d 0.03 g.

^e prepared by solvothermal method.

^f prepared by mechanical stirring.

appeared at 1550 cm⁻¹ and 1422 cm⁻¹ indicate the asymmetric $\nu_{as}(\text{CO}_2)$ and symmetric $\nu_s(\text{CO}_2)$, respectively [76]. Fe-O vibration represents broad bands at 668, 630, 442 cm⁻¹. Besides, the presence of two distinct, typically narrow peaks at 1652 and 1432 cm⁻¹ associated with deprotonation of tetrazolate groups and absence of broadband from 2200 to 2600 cm⁻¹ confirmed the formation of polymer and coordination of N–H of tetrazole groups as described previously. Moreover, our composite exhibits aromatic signals associated with the benzenes ring. Some factors are responsible for the broad characteristic band at 3441 cm⁻¹ such as: OH, stretching vibration owing to the Fe–OH groups, the carboxylic groups of tartaric acid, and adsorbed water (Fig. 3b) [77]. Electron microscopy investigations of the prepared samples (CMNPs/1,4-Zbtb) by three synthetic methods were also performed, extensively. In morphology of the as-prepared composites, we achieved interesting results that were not far from our expectations. Fig. 3c shows a spherical morphology with smooth property and uniform surface for the synthesized CMNPs/1,4-Zbtb by ultrasonic irradiation. As a result, after chiralization, ICP keeps its structural nature and stability in compared to the achiral ICP. But the preparation conditions could affect on the considered structure and its performance. As above mentioned, we also examined CMNPs/1,4-Zbtb synthesis over other methods: mechanical stirring and solvothermal. Fig. 4 shows SEM images of CMNPs/1,4-Zbtb that was synthesized via these synthetic methods for comparative studies. According to morphology images, in mechanical stirring route, CMNPs couldn't well disperse and probably, majority of them deposited on the surface of spheres or mixed together as hybrid material and so CMNPs/1,4-Zbtb could not be core@shell form, completely (Fig. 4c). In addition, solvothermal method had not only the disadvantages of the mechanical route, but also long time to synthesis was another shortcoming in this method (Fig. 4b). All this while, SEM and TEM images of the synthesized CMNPs/1,4-Zbtbs by using ultrasonic irradiation revealed that CMNPs encapsulation was successfully done in

very short time, which agrees well with our previous studies (Fig. 3 and S1) [43–45]. In addition, vibrating-sample magnetometer (VSM) was employed for investigation of magnetic properties of CMNPs/1,4-Zbtb composite. Results indicated that all the samples were superparamagnetic at room temperature and polymeric shell could not suppress their magnetic property (Fig. 3d).

Energy disperse spectroscopy (EDS) [44] as another confirmatory analysis proved the existence of magnetic particles in hollow spherical capsules. In addition, this composite showed high stability in common solvents that PXRD patterns proved (CICP is insoluble in different organic solvents and water) (Fig. S2). Finally, the chiral magnetic composites due to their nature were used in asymmetric Henry reaction as heterogeneous chiral catalysts.

4.2. Catalytic activity for asymmetric Henry reaction

As mentioned above, catalysts with rich basicity can be the efficient catalysts for Henry reaction. So, the activity of CMNPs/1,4-Zbtb and CMNPs/1,3-Zbtb composites was investigated as basic catalysts for this kind of aldol condensation through large numbers of tetrazole nitrogen atoms on the surface of spherical composites. The catalytic experiments were investigated under optimum conditions (solvent, temperature, time and catalyst amount) (Table 1). Before performing the catalytic tests, the stability of CMNPs/1,4-Zbtb in various solvents such as MeOH, EtOH and H₂O was monitored by PXRD (Fig. S2). As shown, these new composites are stable under the essayed conditions for at least 24 h (Fig. S2). To investigate effect of solvent, we examined this transformation in several solvents. EtOH and water gave only 13% and 19% of total yield, respectively. Whereas, a significant acceleration in the rate of reaction and considerable yield were achieved in MeOH, so it was used as an optimized solvent. The influence of temperature was also investigated on the conversion of reaction as main parameter. At first,

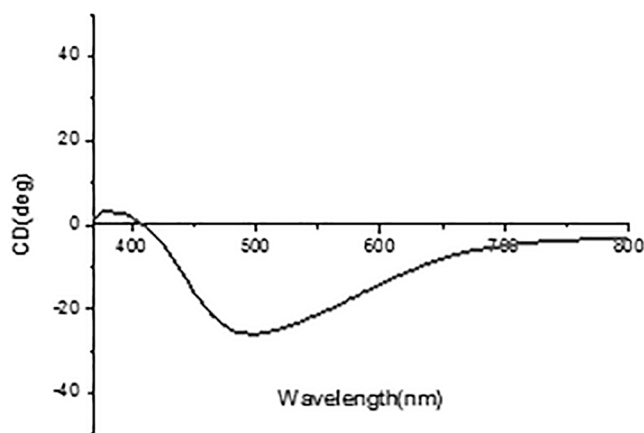


Fig. 5. CD of R-enantiomer of β -nitroalcohol.

temperature 40 °C was examined in the model substrate catalysis that the conversion 20% was achieved (entry 5). Increasing the temperature from 40 to 70 °C could affect on conversion, from 20 to 85% for 12 h. The comparison of composites demonstrated that CMNPs/1,4-Zbtb and CMNPs/1,3-Zbtb catalysts have ability for transformation of aldehyde to chiral alcohol with 85%, 75% conversion and 90%, 85% enantiomeric excess to R enantiomer, respectively (entry 4 and 10). Also, we investigated the hollow achiral form of our catalysts that they had potential to transform benzaldehyde to β -nitroalcohol with 80% (1,4-Zbtb) and 69% (1,3-Zbtb) conversion due to strong interaction between carbonyl groups of aldehyde and catalytic active sites of catalysts surface.

This difference may be attributed to the situation and orientation of the tetrazole groups in polymeric structures (Fig. 1). It seems that the superiority of 1,4-Zbtb to 1,3-Zbtb is due to its structure, physical-chemical properties and more accessible catalytic active centers on its surface. Therefore, it can be concluded that although these composites are almost the same with similar components, but CMNPs/1,4-Zbtb showed higher catalytic activity compared to CMNPs/1,3-Zbtb. After the confirmation of the high performance of 1,4-Zbtb in catalysis, we investigated and compared the activity of the synthesized CICPs that were prepared by three different methods. They have same PXRD patterns but different morphologies that affect on their catalytic activity. The catalytic results show: ultrasonic irradiation > mechanical stirrer > solvothermal (Table 1). This point demonstrates that in ultrasonic method, there are uniform polymeric spherical particles with smooth morphology. In this case, catalytic active sites can be accessed by substrates. Mechanical stirrer and solvothermal processes can be considered as bulk syntheses. According to SEM images, the obtained compounds by these methods are not more regular and do not have high surface area than ultrasonic-assisted synthesis. In fact, using autoclave and synthesis in high pressure and temperature are important agents to produce large capsules with fewer active sites on their surface (35% conversion, 69% ee). Or mechanical stirrer caused the agglomeration of spheres and reducing their active catalytic centers (63% conversion, 78% ee), too. So, it has been concluded that produced CICPs by ultrasonic can show higher activity in basic nitroaldol reaction because a) and they have small size, so rich accessible nitrogen groups as active sites and b) spheres agglomeration is likely much less due to nanoparticles dispersion (owing to presence of ultrasound waves).

About enantiomeric excesses, certainly, in the obtained catalysts by mechanical and solvothermal methods, a high percentage of CMNPs were not encapsulated and probably placed on the outer surface of polymeric particles. To demonstrate the high ability of our chiral catalyst, we compared the activity of CMNPs/1,4-Zbtb with blank sample without any catalyst, 1,4-Zbtb, CMNPs and Fe₃O₄ for reaction between benzaldehyde and nitromethane, too (Fig. 7a). Given that basic groups are considered as the main driving force for this reaction so, there is no

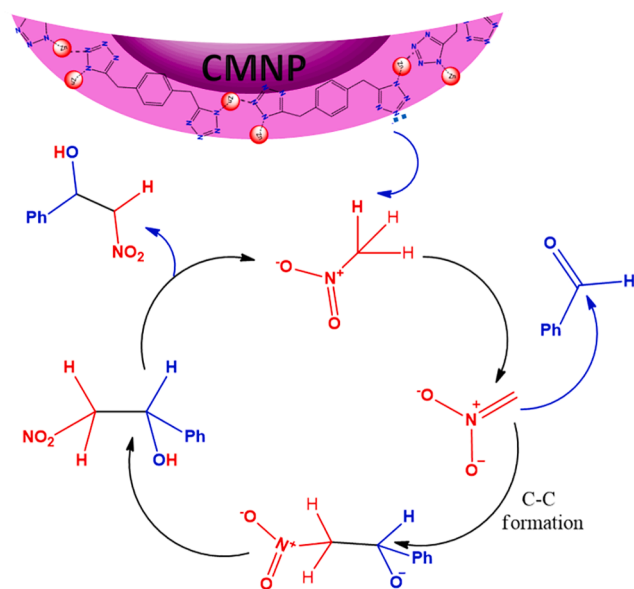


Fig. 6. Proposed catalytic cycle for the formation of a β -nitroalcohol in the Henry reaction catalyzed by CMNPs/1,4-Zbtb.

significant difference in conversions of achiral and chiral spheres as catalyst. Also, due to the influence of acidic catalyst in promotion of Henry reaction, low conversions were also observed for the Fe₃O₄ NPs and CMNPs, although carboxylic groups of tartaric acid led to semi higher result. We know that the nature of substrates has important influence on yields and selectivity. Thus, to show this fact, we compared the reaction of aromatic and aliphatic aldehydes (branched and unbranched) with nitromethane to prepare the respective β -nitroalkanols (yields ranging from 54 to 89% and selectivity up to ca. 90%). Acetaldehyde as an aliphatic aldehyde demonstrated 89% conversion, 63% enantiomeric excess and 75% selectivity. In addition, in comparison to acetaldehyde and isobutyraldehyde, it can be understood that short chain without steric hindrance leads to higher yield and selectivity. Using the same reaction conditions, the obtained nitroalcohol product from the isobutyraldehyde catalysis was isolated in 54% conversion and 70% ee.

This phenomenon is due to the fact that substitution in carbonyl compounds that leads to steric crowding, increasing the activation barrier [78] and reducing the selectivity (60%) [79]. About model substrate, GC analysis with chiral SGE-CYDEX-B capillary column indicated that no further conversion had existed after 12 h and even for 36 h. The obtained results demonstrated the necessity of catalysts for achieving high conversion and enantiomeric excess. As known, the important parameter in the asymmetric catalysis is enantiomeric excess that is used to determine purity of the major chiral isomer with range of 0% to 100%. It is calculated based on following equation:

$$\text{enantiomeric excess} = ee = \frac{A - B}{A + B} \times 100$$

A and B are the enantiomers mass that are determined by the chiral GC data. On the other hand, for investigation of the enantiomeric nature of produced β -nitroalcohol, we utilized CD spectrum in the wavelength range 370–800 nm (Fig. 5) that showed the nature of the obtained enantiomer that was similar to the obtained chiral GC [96] data in this work and CD of R-Limonene.

Interestingly, we observed the change in the kind of enantiomeric excess, from S- to R-enantiomer. Until 5 h, S-enantiomer was the major isomer that was determined with GC but the next 5 h, R-enantiomer was the main isomer. As known, during asymmetric Henry reaction, the racemic mixture of S and R enantiomers of nitroalcohol is produced. In this case, the formation rate and energy of these enantiomers are equal.

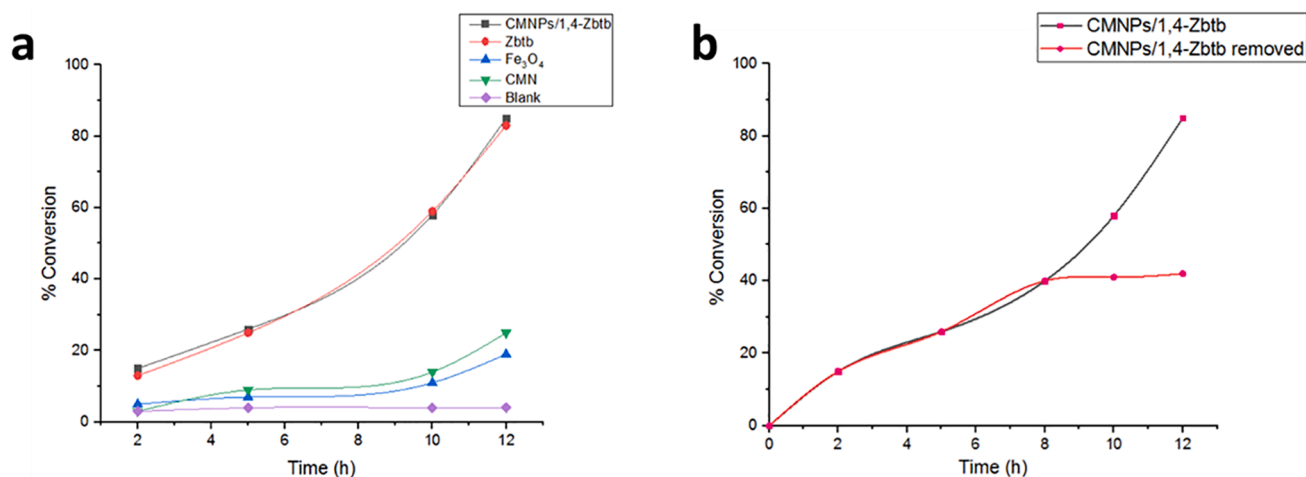


Fig. 7. a) Optimization of catalyst in Henry reaction of benzaldehyde and nitromethane. b) Leaching test confirming no contribution from homogenous catalysis of active species leaching into the reaction solution.

Surely, before or after racemate creation as intermediate, the growth of one enantiomer is seen further, R or S, due to the stability of intermediate and preferred transition state. So far, many examples have been reported with chiral core-shell structures that chiral shell as host entrapped inorganic material as guest. In this case, chirality can be induced from shell to core by various interactions in confined space [80,81]. In this respect, we believe that similar interaction has occurred in the opposite direction (chirality information transfer from core to shell by the same interactions). One of the works has been done in this area was about chirality activity of unprotected Au₂₈ and Au₅₅. Gold cluster was intrinsically chiral due to the stability in energy state. In the second step, in comparison of bare gold cluster with protected manner, it was found that protection by methylthiol monolayer can enhance the degree of chirality of the metallic core. It is suggested that interaction between chiral core and achiral shell is responsible for chirality induction from metal center to ligand [82,83]. About mechanism, recently we published a work about the basic effect of nitrogen groups for promoting Henry reaction [61]. Similarly, in this work it should be said that the most prevalent mechanism for Henry reaction is based on the deprotonating of nitroalkane under basic condition. In second step, C-C bond is formed upon nucleophilic addition and subsequently β -nitroalkanol is produced by means of protonation [79]. In our report for the evaluation of the mechanism and stereoselectivity, we must suppose several hypotheses, first N moieties of tetrazole would deprotonate nitromethane, so in the next step, bidentate nature of nitronate anions as hydrogen-bond acceptor led to the formation of chiral tetrazolium nitroate ion pair. Eventually, nucleophilic addition has occurred in high stereoselectivity manner. It can be concluded that responsibility for the second sequence, is N-H...O as non-covalent interactions. Moreover, we suggest that other interactions like C-H... π has an auxiliary role in stabilizing the transition state (TS) and increasing the reaction rate that the way π system of the phenyl scaffold can activate aldehyde through C-H... π interaction and subsequently affect the transition state (Fig. 6). To illustrate protection power and to determine heterogeneity of our composite, the leaching test of active species into the catalytic reaction medium was carried out. After 8 h and removal of catalyst from reaction mixture, the acquired results demonstrated that catalyst was necessary to promote the reaction (Fig. 7b).

4.3. Catalytic activity for oxidation of alcohols

In the field of oxidation of alcohols to achieve carbonyl compounds, the best way is using non-precious and environmentally friendly precursors. Except for oxidant-free photocatalytic instances, it is well known that the oxidation processes can be occurred in the presence of

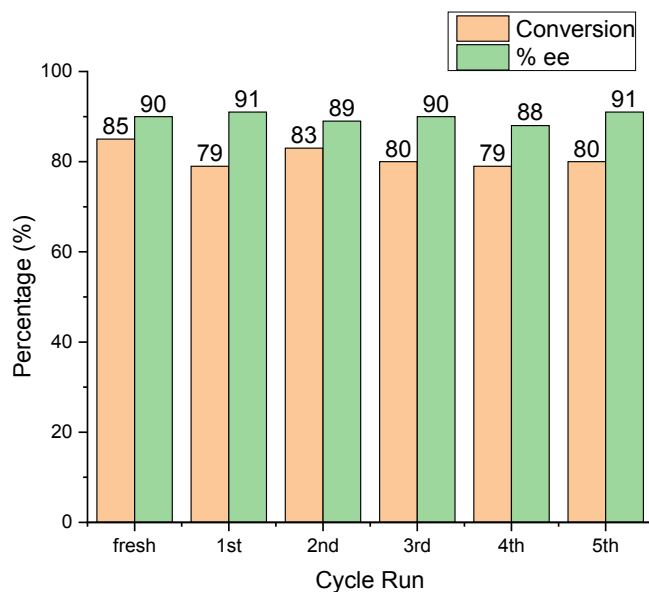


Fig. 8. Catalytic cycles for asymmetric Henry reaction of benzaldehyde and nitromethane catalyzed by CMNPs/1,4-Zbtb (5 mol %). Reaction conditions: benzaldehyde (2 mmol), nitromethane (5 mmol) in 5 mL of MeOH at 70 °C.

the various oxidants in most cases normally [84]. Among them, hydrogen peroxide can be used as an ideal green oxidant due to its low cost, high content of active oxygen, non-toxic and corrosive. On the other hand, Zinc as an easily available metal is relatively inexpensive and non-toxic than precious metals (mostly Pd, Ir, Ru, and Au) which makes it as a catalyst for practical applications particularly on an industrial scale [85]. In addition to, the role of metal in oxidation [86], we can suggest that tetrazole groups of btmbenzene can act as a base. In this state, tetrazole moieties as weak bases can promote oxidation of alcohols through generating alkoxy [87]. The benzaldehyde is produced by optimized 1,4-Zbtb (prepared in the ultrasonic bath) through oxidizing benzylalcohol in the presence of H₂O₂. After evaluation of H₂O₂ amount (Fig. S6), the optimal combination is achieved by applying four equivalents of H₂O₂ (in three portions). This reaction (benzylalcohol to benzaldehyde) was also performed in H₂O as the green solvent with low percent yield (35%). Successive adding of H₂O₂ improved the yield but increasing the temperature decreased it. The mechanism of the conversion of alcohols to aldehyde in the presence of H₂O₂ as oxidant and

Table 2

Comparison of CMNPs/1,4-Zbtb as a chiral heterogeneous catalyst with the other chiral catalysts in the asymmetric Henry reaction.

Entry	Catalyst	Condition	Aldehyde	Yield (%)	Ee (%)	Ref.
1	[Cd ₂ (Cu(salan))(DMF) ₃]	MeOH/DIPEA/45 °C/48 h	Benzaldehyde	71	95	[91]
2	CPs S-3b	DCM-THF/NaOAc/25 °C/24 h	Benzaldehyde	85	70	[69]
3	Microporous polyurethane (MPU)	5 mol%/MeOH/50 °C/10 h	Benzaldehyde	0	0	[92]
4	Chiral-Ni-Schiff Base encapsulated Inside Zeolite-Y	-10 °C/Ethanol/MW/15 min	Benzaldehyde	89	78	[93]
5	Salen-lignd/Cu(OAc) ₂ ·H ₂ O	H ₂ O/35 °C/72 h	Benzaldehyde	69	69	[89]
6	Copper(II)-salen complexes	MeOH/RT/30 h	Benzaldehyde	56	56	[94]
7	[Zn ₂ (L1) ₂ (4,4'-bipyridine) ₂ (H ₂ O)(DMF)] _n	MeOH/70 °C/48 h	4-nitro benzaldehyde	84	71	[95]
8	Pd@CCOF-MPC	EtOH/K ₂ CO ₃ /25 °C/8 h	Benzaldehyde	97	95	[90]
9	CMNPs/1,4-Zbtb	MeOH/70 °C/12 h	Benzaldehyde	85	90	This work

Zinc(II) as catalyst has been investigated by computational methods in literatures [88]. In the transition state, O-O bond in H₂O₂ is weakened and coordinated to Zinc at the surface of spheres. These weak O-O bonds are replaced by strong O-H bonds that are also coordinated to Zinc atoms. The generated water molecules as by-product have interactions with aldehyde molecules by hydrogen bonding. Also, they can accelerate separation of aldehyde molecules from metals. Finally, the control experiment was investigated without catalyst that no progress was seen in the catalytic reaction. Given that the importance of asymmetric Henry reaction and its chiral product, chiral 1,3-Zbtb composite was also investigated in this kind of asymmetric catalysis but it showed lower activity than 1,4-Zbtb composite (main catalyst) so, we did not study its applicative application in oxidation of alcohols. Although, we should remind that 1,3-Zbtb composite showed moderate to poor performance as Lewis-acid in Michael reaction [45].

4.4. Catalyst recyclability

Due to significance of the recycling and life-time of heterogeneous catalysts in practical applications, we investigated recyclability of the optimized CMNPs/1,4-Zbtb catalyst. Investigations showed high stability of catalyst with less chiral species leaching after 5 catalytic consecutive cycles. Not only no significant deactivation was observed, even after the fifth cycle but also both high conversion and enantiomeric excess (ee) are observed due to high stability of catalyst along with high protection of CMNPs (Fig. 8). PXRD, SEM, VSM and ICP analysis showed that our sphere-like composite is stable chiral heterogeneous catalyst (Figs. S2, S3, S4, S5). These observations can confirm a) protection of CMNPs by stable polymeric shell and b) the presence of accessible tetrazole groups as catalytic active sites after several cycles. Since, robust shell prevents leaching of CMNPs so, enantioselectivity does not significantly decrease. In general, it can be said that the strength and capability of our polymer are at a very high level compared to other mineral and organic polymers. Also, to compare our catalyst with reported heterogeneous and homogeneous catalysts in asymmetric Henry reaction, Table 2 has been presented. Although, relatively good results have been obtained by other catalysts, but the high cost of the used compounds in their synthesis is a fault. For example, Pd NPs and salen-ligands can be mentioned that they limit the use of the synthesized catalysts, in addition long time of catalytic reactions in high or very low temperature that they are main disadvantages of these kinds of catalysts [89,90].

5. Conclusion

In conclusion, we reported the first examples of the CMNPs/(1,3- and 1,4-)Zbtb core-shell microspheres as promising chiral magnetic spherical polymers via ultrasonic-assisted encapsulation as an effective method. In this synthetic way, chiral magnetic nanoparticles could enter into spherical polymers that due to this process, chirality induction happened from chiral magnetic core to optically inactive polymeric shell through hydrogen-bonding interactions. These compositionally

modified polymers by using chiral magnetic nanoparticles showed their capability for enantioselective conversion of aldehydes to chiral alcohols. Catalytic results demonstrated that CMNPs/1,4-Zbtb is better than CMNPs/1,3-Zbtb due to the orientation of the side groups (basic centers) around the benzene ring that has a vital role to convert CMNPs/1,4-Zbtb to optimized catalyst. The other synthetic methods were examined to produce optimized CICIP (CMNPs/1,4-Zbtb). The important point is that the synthesis method could directly affect on catalysis performance of polymers. The obtained samples by solvothermal and mechanical stirring did not show high catalytic activity than ultrasonic synthesis. An important property of this hollow catalytic system is high protection of chiral components without any change in chemical structure of the polymer.

With the presence of the nitrogen and unsaturated Zn atoms as basic and acidic active sites at the surface of shell, magnetic and chirality property, our sustainable composite showed ability in nitroaldol (asymmetric) condensation and oxidative transformation of alcohol to aldehyde with high performance (mild catalytic conditions). Also, other unique advantages of our green catalyst as a low-cost chiral catalyst are high stability, reusing for five successive runs with retention of structure and morphology without obvious loss of activity. So, it is unprecedented among other chiral polymeric catalysts. Our methodology will be able to induce chirality into other hollow structures, especially metal-organic materials. Finally, given its efficiency, we highly expect that this kind of asymmetric catalytic system can have an immediate impact on the asymmetric syntheses and catalysis.

Declaration of Competing Interest

The authors declare that they have no known competing financial interests or personal relationships that could have appeared to influence the work reported in this paper.

Acknowledgment

Support for this investigation by Tarbiat Modares University is gratefully acknowledged.

Appendix A. Supplementary data

Supplementary data to this article can be found online at <https://doi.org/10.1016/j.ultsonch.2021.105499>.

References

- [1] J. Chin, S.S. Lee, K.J. Lee, S. Park, D.H. Kim, A metal complex that binds α -amino acids with high and predictable stereospecificity, *Nature* 401 (1999) 254–257.
- [2] L. Ma, C. Abney, W. Lin, Enantioselective catalysis with homochiral metal-organic frameworks, *Chem. Soc. Rev.* 38 (2009) 1248–1256, <https://doi.org/10.1039/b807083k>.
- [3] L. Ma, J.M. Falkowski, C. Abney, W. Lin, A series of isorecticular chiral metal-organic frameworks as a tunable platform for asymmetric catalysis, *Nat. Chem.* 2 (2010) 838–846.
- [4] L. Zhang, R. Clérac, P. Heijboer, W. Schmitt, Influencing the Symmetry of High-Nuclearity and High-Spin Manganese Oxo Clusters: Supramolecular Approaches to

- Manganese-Based Keplerates and Chiral Solids, *Angew. Chem. Int. Ed.* 51 (2012) 3007–3011.
- [5] Y. Liu, W. Xuan, Y. Cui, Engineering homochiral metal-organic frameworks for heterogeneous asymmetric catalysis and enantioselective separation, *Adv. Mater.* 22 (2010) 4112–4135.
- [6] G. Novitski, G. Pilet, L. Ungur, V.V. Moshchalkov, W. Wernsdorfer, L.F. Chibotaru, D. Luneau, A.K. Powell, Heterometallic CuII/DyIII 1D chiral polymers: chirogenesis and exchange coupling of toroidal moments in trinuclear Dy3 single molecule magnets, *Chem. Sci.* 3 (2012) 1169–1176, <https://doi.org/10.1039/C2SC00728B>.
- [7] Y. Peng, T. Gong, K. Zhang, X. Lin, Y. Liu, J. Jiang, Y. Cui, Engineering chiral porous metal-organic frameworks for enantioselective adsorption and separation, *Nat. Commun.* 5 (2014) 1–9, <https://doi.org/10.1038/ncomms5406>.
- [8] S.-Y. Zhang, D. Li, D. Guo, H. Zhang, W. Shi, P. Cheng, L. Wojtas, M.J. Zaworotko, Synthesis of a chiral crystal form of MOF-5, CMOF-5, by chiral induction, *J. Am. Chem. Soc.* 137 (2015) 15406–15409.
- [9] D. Dang, P. Wu, C. He, Z. Xie, C. Duan, Homochiral metal-organic frameworks for heterogeneous asymmetric catalysis, *J. Am. Chem. Soc.* 132 (2010) 14321–14323.
- [10] M. Banerjee, S. Das, M. Yoon, J.C. Hee, H.H. Myung, M.P. Se, G. Seo, O. Kim, Postsynthetic modification switches an achiral framework to catalytically active homochiral metal-organic porous materials, *J. Am. Chem. Soc.* 131 (2009) 7524–7525, <https://doi.org/10.1021/ja901440g>.
- [11] Y. Yang, X.-L. Pei, Q.-M. Wang, Postclustering dynamic covalent modification for chirality control and chiral sensing, *J. Am. Chem. Soc.* 135 (2013) 16184–16191.
- [12] X. Zhao, M. Wong, C. Mao, T.X. Trieu, J. Zhang, P. Feng, X. Bu, Size-selective crystallization of homochiral camphorate metal-organic frameworks for lanthanide separation, *J. Am. Chem. Soc.* 136 (2014) 12572–12575.
- [13] M. Zhou, E.-S.M. El-Sayed, Z. Ju, W. Wang, D. Yuan, The synthesis and applications of chiral pyrrolidine functionalized metal-organic frameworks and covalent-organic frameworks, *Inorg. Chem. Front.* 7 (2020) 1319–1333.
- [14] L. Pérez-García, D.B. Amabilino, Spontaneous resolution, whence and whither: from enantiomorphous solids to chiral liquid crystals, monolayers and macro- and supra-molecular polymers and assemblies, *Chem. Soc. Rev.* 36 (2007) 941–967.
- [15] J. Hou, M. Li, Z. Li, S. Zhan, X. Huang, D. Li, Supramolecular Helix-to-Helix Induction: A 3D Anionic Framework Containing Double-Helical Strands Templated by Cationic Triple-Stranded Cluster Helicates, *Angew. Chem.* 120 (2008) 1735–1738.
- [16] E.-Q. Gao, Y.-F. Yue, S.-Q. Bai, Z. He, C.-H. Yan, From Achiral Ligands to Chiral Coordination Polymers: Spontaneous Resolution, Weak Ferromagnetism, and Topological Ferrimagnetism, *J. Am. Chem. Soc.* 126 (2004) 1419–1429, <https://doi.org/10.1021/ja039104a>.
- [17] H. Wang, Z. Chang, Y. Li, R.-M. Wen, X.-H. Bu, Chiral uranyl-organic compounds assembled with achiral furandicarboxylic acid by spontaneous resolution, *Chem. Commun.* 49 (2013) 6659–6661.
- [18] B. Liu, H.-F. Zhou, L. Hou, Z. Zhu, Y.-Y. Wang, A chiral metal-organic framework with polar channels: unique interweaving six-fold helices and high CO₂/CH₄ separation, *Inorg. Chem. Front.* 3 (2016) 1326–1331.
- [19] W. Zhang, Y. Zhao, L. Yin, Chiral solvation induced supramolecular chiral assembly of achiral polymers, in: *Molecular self-assembly in nanoscience and nanotechnology*, InTech Rijeka, 2017.
- [20] R.E. Morris, X. Bu, Induction of chiral porous solids containing only achiral building blocks, *Nat. Chem.* 2 (2010) 353–361, <https://doi.org/10.1038/nchem.628>.
- [21] C. Li, M. Numata, A.-H. Bae, K. Sakurai, S. Shinkai, Self-assembly of supramolecular chiral insulated molecular wire, *J. Am. Chem. Soc.* 127 (2005) 4548–4549.
- [22] E. Yashima, N. Ousaka, D. Taura, K. Shimomura, T. Ikai, K. Maeda, Supramolecular helical systems: helical assemblies of small molecules, foldamers, and polymers with chiral amplification and their functions, *Chem. Rev.* 116 (2016) 13752–13990.
- [23] K. Shimomura, T. Ikai, S. Kanoh, E. Yashima, K. Maeda, Switchable enantioselective separation based on macromolecular memory of a helical polyacetylene in the solid state, *Nat. Chem.* 6 (2014) 429.
- [24] X. Yang, S. Yuan, L. Zou, H. Drake, Y. Zhang, J. Qin, A. Alsahme, H. Zhou, One-Step Synthesis of Hybrid Core-Shell Metal-Organic Frameworks, *Angew. Chem.* 130 (2018) 3991–3996.
- [25] K. Berijani, A. Morsali, J.T. Hupp, An effective strategy for creating asymmetric MOFs for chirality induction: a chiral Zr-based MOF for enantioselective epoxidation, *Catal. Sci. Technol.* 9 (2019) 3388–3397.
- [26] K. Berijani, A. Morsali, Dual activity of durable chiral hydroxyl-rich MOF for asymmetric catalytic reactions, *J. Catal.* 378 (2019) 28–35.
- [27] K. Berijani, A. Morsali, Construction of an Asymmetric Porphyrinic Zirconium Metal-Organic Framework through Ionic Postchiral Modification, *Inorg. Chem.* (2020), <https://doi.org/10.1021/acs.inorgchem.0c02811>.
- [28] S.H.A.M. Leenders, R. Gramage-Doria, B. de Bruin, J.N.H. Reek, Transition metal catalysis in confined spaces, *Chem. Soc. Rev.* 44 (2015) 433–448.
- [29] Y. Liu, Z. Tang, Multifunctional nanoparticle@MOF core-shell nanostructures, *Adv. Mater.* 25 (2013) 5819–5825.
- [30] P. Hu, J.V. Morabito, C.-K. Tsung, Core-shell catalysts of metal nanoparticle core and metal-organic framework shell, *ACS Catal.* 4 (2014) 4409–4419.
- [31] L. Chen, H. Chen, Y. Li, One-pot synthesis of Pd@MOF composites without the addition of stabilizing agents, *Chem. Commun.* 50 (2014) 14752–14755.
- [32] M. Oh, C.A. Mirkin, Chemically tailorable colloidal particles from infinite coordination polymers, *Nature* 438 (2005) 651–654.
- [33] M. Oh, C.A. Mirkin, Ion exchange as a way of controlling the chemical compositions of nano- and microparticles made from infinite coordination polymers, *Angew. Chem. Int. Ed.* 45 (2006) 5492–5494.
- [34] S. Jung, M. Oh, Monitoring shape transformation from nanowires to nanocubes and size-controlled formation of coordination polymer particles, *Angew. Chem.* 120 (2008) 2079–2081.
- [35] H. Wei, B. Li, Y. Du, S. Dong, E. Wang, Nucleobase-metal hybrid materials: Preparation of submicrometer-scale, spherical colloidal particles of adenine-gold (III) via a supramolecular hierarchical self-assembly approach, *Chem. Mater.* 19 (2007) 2987–2993.
- [36] K.H. Park, K. Jang, S.U. Son, D.A. Sweigart, Self-supported organometallic rhodium quinonoid nanocatalysts for stereoselective polymerization of phenylacetylene, *J. Am. Chem. Soc.* 128 (2006) 8740–8741.
- [37] A. Gheorghie, M.A. Tepaske, S. Tanase, Homochiral metal-organic frameworks as heterogeneous catalysts, *Inorg. Chem. Front.* 5 (2018) 1512–1523.
- [38] Y.-M. Jeon, J. Heo, C.A. Mirkin, Dynamic Interconversion of Amorphous Microparticles and Crystalline Rods in Salen-Based Homochiral Infinite Coordination Polymers, *J. Am. Chem. Soc.* 129 (2007) 7480–7481, <https://doi.org/10.1021/ja071046w>.
- [39] E. Yashima, K. Maeda, H. Iida, Y. Furusho, K. Nagai, Helical polymers: synthesis, structures, and functions, *Chem. Rev.* 109 (2009) 6102–6211.
- [40] M. Reggelin, M. Schultz, M. Holbach, Helical chiral polymers without additional stereogenic units: a new class of ligands in asymmetric catalysis, *Angew. Chem. Int. Ed.* 41 (2002) 1614–1617.
- [41] E. Yashima, K. Maeda, Chirality-responsive helical polymers, *Macromolecules* 41 (2008) 3–12.
- [42] X. Lin, B. Liu, H. Huang, C. Shi, Y. Liu, Z. Kang, One-step synthesis of ZnS-N/C nanocomposites derived from Zn-based chiral metal-organic frameworks with highly efficient photocatalytic activity for the selective oxidation of cis-cyclooctene, *Inorg. Chem. Front.* 5 (2018) 723–731.
- [43] Z. Sharifzadeh, S. Abedi, A. Morsali, Fabrication of novel multi-morphological tetrazole-based infinite coordination polymers; transformation studies and their calcination to mineral zinc oxide nano- and microarchitectures, *J. Mater. Chem. A* 2 (2014) 4803–4810.
- [44] R. Nouri, S. Abedi, A. Morsali, Design and synthesis of two novel functional metal-organic microcapsules; an investigation into ligand expansion effects on the metal-organic microcapsules' properties, *RSC Adv.* 6 (2016) 101652–101659.
- [45] R. Nouri, S. Abedi, A. Morsali, A novel synthesis route for preparation of tetrazole-based infinite coordination polymers and their application as an efficient catalyst for Michael addition reactions, *J. Iran. Chem. Soc.* 14 (2017) 1601–1612.
- [46] S.Y. Hao, X.G. Ma, G.H. Cui, Ultrasonic synthesis of two nanostructured cadmium (II) coordination supramolecular polymers: Solvent influence, luminescence and photocatalytic properties, *Ultrason. Sonochem.* 37 (2017) 414–423.
- [47] K.S. Suslick, S.-B. Choe, A.A. Cichowlas, M.W. Grinstaff, Sonochemical synthesis of amorphous iron, *Nature* 353 (1991) 414–416.
- [48] A. Afzalnia, A. Mirzaei, A. Nikseresh, T. Musabeygi, Ultrasound-assisted oxidative desulfurization process of liquid fuel by phosphotungstic acid encapsulated in a interpenetrating amine-functionalized Zn (II)-based MOF as catalyst, *Ultrason. Sonochem.* 34 (2017) 713–720.
- [49] F. Li, C. Xie, Z. Cheng, H. Xia, Ultrasound responsive block copolymer micelle of poly (ethylene glycol)-poly (propylene glycol) obtained through click reaction, *Ultrason. Sonochem.* 30 (2016) 9–17.
- [50] K.S. Suslick, *Sonochemistry, Science* 247 (1990) 1439–1445.
- [51] C. Vaitis G. Sourkouni C. Argiris Metal Organic Frameworks (MOFs) and ultrasound: A review *Ultrason. Sonochem.* 52 2019 106119 <https://doi.org/https://doi.org/10.1016/j.ultrsonch.2018.11.004>.
- [52] N.N. Gharat, V.K. Rathod, Chapter 1 - Ultrasound-assisted organic synthesis, in: Inamuddin, R. Boddula, A.M.B.T.-G.S.P. for C. and E.E. and S. Asiri (Eds.), Elsevier, 2020: pp. 1–41. <https://doi.org/https://doi.org/10.1016/B978-0-12-819540-6.00001-2>.
- [53] R.B.N. Baig, R.S. Varma, Alternative energy input: mechanochemical, microwave and ultrasound-assisted organic synthesis, *Chem. Soc. Rev.* 41 (2012) 1559–1584, <https://doi.org/10.1039/C1CS15204A>.
- [54] G. Sargazi D. Afzali N. Daldosso H. Kazemian N.P.S. Chauhan Z. Sadeghian T. Tajerian A. Ghafarinazari M. Mozafari A systematic study on the use of ultrasound energy for the synthesis of nickel-metal organic framework compounds *Ultrason. Sonochem.* 27 (2015) 395402 <https://doi.org/https://doi.org/10.1016/j.ultrsonch.2015.04.004>.
- [55] E. Haque S.H. Jung Synthesis of isostructural metal-organic frameworks, CPO-27s, with ultrasound, microwave, and conventional heating: Effect of synthesis methods and metal ions, *Chem. Eng. J.* 173 (2011) 866872 <https://doi.org/https://doi.org/10.1016/j.cej.2011.08.037>.
- [56] M.D. Luque de Castro F. Priego-Capote Ultrasound-assisted crystallization (sonocrystallization), *Ultrason. Sonochem.* 14 (2007) 717724 <https://doi.org/https://doi.org/10.1016/j.ultrsonch.2006.12.004>.
- [57] A.R. Abbasi K. Akhbari A. Morsali Dense coating of surface mounted CuBTC Metal-Organic Framework nanostructures on silk fibers, prepared by layer-by-layer method under ultrasound irradiation with antibacterial activity *Ultrason. Sonochem.* 19 (2012) 846852 <https://doi.org/https://doi.org/10.1016/j.ultrsonch.2011.11.016>.
- [58] A. Nikseresh, A. Daniyali, M. Ali-Mohammadi, A. Afzalnia, A. Mirzaei, Ultrasound-assisted biodiesel production by a novel composite of Fe (III)-based MOF and phosphotungstic acid as efficient and reusable catalyst, *Ultrason. Sonochem.* 37 (2017) 203–207.
- [59] A. Mirzaei, T. Musabeygi, A. Afzalnia, Sonochemical synthesis of magnetic responsive Fe₃O₄@TMU-17-NH₂ composite as sorbent for highly efficient ultrasonic-assisted denitrogenation of fossil fuel, *Ultrason. Sonochem.* 38 (2017) 664–671.

- [60] S.S. Nadar, V.K. Rathod, Encapsulation of lipase within metal-organic framework (MOF) with enhanced activity intensified under ultrasound, *Enzyme Microb. Technol.* 108 (2018) 11–20.
- [61] S.A.A. Razavi, K. Berijani, A. Morsali, Hybrid nanomaterials for asymmetric purposes: green enantioselective C-C bond formation by chiralization and multifunctionalization approaches, *Catalysis, Sci. Tech.* (2020).
- [62] T. Yamada, K. Narasaka, Asymmetric oxidation of olefins with osmium tetroxide coordinated by chiral diamines derived from L-tartaric acid, *Chem. Lett.* 15 (1986) 131–134.
- [63] R.B.N. Baig, M.N. Nadagouda, R.S. Varma, Magnetically retrievable catalysts for asymmetric synthesis, *Coord. Chem. Rev.* 287 (2015) 137–156.
- [64] M.O. Lorenzo, S. Haq, T. Bertrams, P. Murray, R. Raval, C.J. Baddeley, Creating chiral surfaces for enantioselective heterogeneous catalysis: R, R-tartaric acid on Cu (110), *J. Phys. Chem. B* 103 (1999) 10661–10669.
- [65] R. Abazari A.R. Mahjoub S. Molaie F. Ghaffarifar E. Ghasemi A.M.Z. Slawin C.L. Carpenter-Warren The effect of different parameters under ultrasound irradiation for synthesis of new nanostructured Fe₃O₄@bio-MOF as an efficient anti-leishmanial in vitro and in vivo conditions *Ultrason. Sonochem.* 43 (2018) 248261 <https://doi.org/https://doi.org/10.1016/j.ultsonch.2018.01.022>.
- [66] N.M. Mahmoodi M. Oveisi A. Taghizadeh M. Taghizadeh Novel magnetic amine functionalized carbon nanotube/metal-organic framework nanocomposites: From green ultrasound-assisted synthesis to detailed selective pollutant removal modelling from binary systems *J. Hazard. Mater.* 368 (2019) 746759 <https://doi.org/https://doi.org/10.1016/j.jhazmat.2019.01.107>.
- [67] T. Karasawa, R. Oriz, N. Kumagai, M. Shibasaki, Anti-selective catalytic asymmetric nitroaldol reaction of α -keto esters: Intriguing solvent effect, flow reaction, and synthesis of active pharmaceutical ingredients, *J. Am. Chem. Soc.* 140 (2018) 12290–12295.
- [68] T. Marcelli, R.N.S. van der Haas, J.H. van Maarseveen, H. Hiemstra, Asymmetric organocatalytic Henry reaction, *Angew. Chem. Int. Ed.* 45 (2006) 929–931.
- [69] V.A. Larionov L.V. Yashkina A.F. Smol'yakov, Y. V Zubavichus, K.K. Babievsky, N. V Akat'yev, A.A. Titov, Y.N. Belokon, V.I. Maleev, Synthesis and investigations of chiral NNO type copper (II) coordination polymers, *Chem. Select.* 3 (2018) 653656.
- [70] K. Berijani H. Hosseini-Monfared Collaborative effect of Mn-porphyrin and mesoporous SBA-15 in the enantioselective epoxidation of olefins with oxygen *Inorgan. Chim. Acta.* 471 (2018) 113120 <https://doi.org/https://doi.org/10.1016/j.ica.2017.10.037>.
- [71] A.E. Mattson, Tricks for noncovalent catalysis, *Science* 358 (2017) 720.
- [72] J.D. White, S. Shaw, A new catalyst for the asymmetric Henry reaction: synthesis of β -nitroethanols in high enantiomeric excess, *Org. Lett.* 14 (2012) 6270–6273.
- [73] K. Kodama, K. Sugawara, T. Hirose, Synthesis of Chiral 1, 3-diamines derived from cis-2-benzamidocyclohexanecarboxylic acid and their application in the catalyzed enantioselective Henry reaction, *Chem. A Europ. J.* 17 (2011) 13584–13592.
- [74] J. Zheng, Y. Dong, W. Wang, Y. Ma, J. Hu, X. Chen, X. Chen, In situ loading of gold nanoparticles on Fe₃O₄@ SiO₂ magnetic nanocomposites and their high catalytic activity, *Nanoscale.* 5 (2013) 4894–4901.
- [75] K. Moovendaran, V. Jayaramkrishnan, S. Natarajan, Optical studies on L-tartaric acid and L-prolinium tartrate, *Photon. Optoelec.* 3 (2014).
- [76] W. Li, B. Zhang, X. Li, H. Zhang, Q. Zhang, Preparation and characterization of novel immobilized Fe₃O₄@ SiO₂@ mSiO₂-Pd (0) catalyst with large pore-size mesoporous for Suzuki coupling reaction, *Appl. Catal. A* 459 (2013) 65–72.
- [77] L. Hadian-Dehkordi, H. Hosseini-Monfared, Enantioselective aerobic oxidation of olefins by magnetite nanoparticles at room temperature: a chiral carboxylic acid strategy, *Green Chem.* 18 (2016) 497–507.
- [78] P. Hammar, T. Marcelli, H. Hiemstra, F. Himo, Density functional theory study of the cinchona thiourea-catalyzed Henry reaction: mechanism and enantioselectivity, *Adv. Synth. Catal.* 349 (2007) 2537–2548.
- [79] R. Ballini, G. Bosica, Nitroaldol reaction in aqueous media: An important improvement of the Henry reaction, *J. Organ. Chem.* 62 (1997) 425–427.
- [80] P.D. Jadzinsky, G. Calero, C.J. Ackerson, D.A. Bushnell, R.D. Kornberg, Structure of a thiol monolayer-protected gold nanoparticle at 1.1 Å resolution, *Science* 318 (2007) 430–433.
- [81] K.C. Bentz, D.A. Savin, Hollow polymer nanocapsules: synthesis, properties, and applications, *Polym. Chem.* 9 (2018) 2059–2081.
- [82] C. Noguez, I.L. Garzón, Optically active metal nanoparticles, *Chem. Soc. Rev.* 38 (2009) 757–771.
- [83] I.L. Garzón, M.R. Beltrán, G. González, I. Gutierrez-González, K. Michaelian, J. A. Reyes-Nava, J.I. Rodriguez-Hernández, Chirality, defects, and disorder in gold clusters, the European physical Journal d-atomic, molecular, optical and plasma, *Physics.* 24 (2003) 105–109.
- [84] K. Shimizu, K. Kon, K. Shimura, S.S.M.A. Hakim, Acceptor-free dehydrogenation of secondary alcohols by heterogeneous cooperative catalysis between Ni nanoparticles and acid–base sites of alumina supports, *J. Catal.* 300 (2013) 242–250.
- [85] X. Wu, A general and efficient zinc-catalyzed oxidation of benzyl alcohols to aldehydes and esters, *Chem. A Europ. J.* 18 (2012) 8912–8915.
- [86] X. Wu, Toward greener oxidative transformations: base-metal catalysts and metal-free reactions, *The Chemical Record.* 15 (2015) 949–963.
- [87] E.T.T. Kumpulainen, A.M.P. Koskinen, Catalytic activity dependency on catalyst components in aerobic copper–TEMPO oxidation, *Chem. A Europ. J.* 15 (2009) 10901–10911.
- [88] R.U. Nisa, T. Mahmood, R. Ludwig, K. Ayub, Theoretical mechanistic investigation of zinc (II) catalyzed oxidation of alcohols to aldehydes and esters, *RSC Adv.* 6 (2016) 31876–31883.
- [89] A. Dixit, P. Kumar, S. Singh, Synthesis of chiral salalen ligands and their in-situ generated Cu-complexes for asymmetric Henry reaction, *Chirality* 30 (2018) 1257–1268.
- [90] H.-C. Ma, J.-L. Kan, G.-J. Chen, C.-X. Chen, Y.-B. Dong, Pd NPs-loaded homochiral covalent organic framework for heterogeneous asymmetric catalysis, *Chem. Mater.* 29 (2017) 6518–6524.
- [91] Y. Fan, Y. Ren, J. Li, C. Yue, H. Jiang, Enhanced activity and enantioselectivity of Henry reaction by the postsynthetic reduction modification for a chiral Cu (salen)-based metal–organic framework, *Inorg. Chem.* 57 (2018) 11986–11994.
- [92] S.K. Dey, N. de Sousa Amadeu, C. Janiak, Microporous polyurethane material for size selective heterogeneous catalysis of the Knoevenagel reaction, *Chem. Commun.* 52 (2016) 7834–7837.
- [93] M. Sharma, B. Das, G.V. Karunakar, L. Satyanarayana, K.K. Bania, Chiral Ni-schiff base complexes inside zeolite-Y and their application in asymmetric Henry reaction: effect of initial activation with microwave irradiation, *J. Phys. Chem. C.* 120 (2016) 13563–13573.
- [94] A. Das, R.I. Kureshy, P.S. Subramanian, H.K. Noor-ul, S.H.R. Abdi, H.C. Bajaj, Synthesis and characterization of chiral recyclable dimeric copper (II)-salen complexes and their catalytic application in asymmetric nitroaldol (Henry) reaction, *Catal. Sci. Technol.* 4 (2014) 411–418.
- [95] A. Karmakar, M.F.C. Guedes da Silva, A.J.L. Pombeiro, Zinc metal–organic frameworks: efficient catalysts for the diastereoselective Henry reaction and transesterification, *Dalton Trans.* 43 (2014) 7795–7810, <https://doi.org/10.1039/C4DT00219A>.
- [96] M. Fujiki, Y. Kawagoe, Y. Nakano, A. Nakao, Mirror-symmetry-breaking in poly [(9,9-di-n-octylfluorenyl)-2,7-diyl]-alt-biphenyl] (PF8P2) is susceptible to terpene chirality, achiral solvents, and mechanical stirring, *Molecules* (Basel, Switzerland) 18 (6) (2013) 7035–7057, <https://doi.org/10.3390/molecules18067035>. In press.